Test of the fluctuation theorem for single-electron transport

B. Küng, C. Rössler, M. Beck, M. Marthaler, D. S. Golubev et al.

Additional information on J. Appl. Phys.

Test of the fluctuation theorem for single-electron transport

B. Küng,[1,a)] C. Rössler,[1] M. Beck,[2] M. Marthaler,[3] D. S. Golubev,[4] Y. Utsumi,[5] T. Ihn,[1] and K. Ensslin[1]

[1]*Solid State Physics Laboratory, ETH Zurich, 8093 Zurich, Switzerland*
[2]*Institute for Quantum Electronics, ETH Zurich, 8093 Zurich, Switzerland*
[3]*Institut für Theoretische Festkörperphysik and DFG Center for Functional Nanostructures (CFN), Karlsruhe Institute of Technology, 76128 Karlsruhe, Germany*
[4]*Institut für Nanotechnologie, Karlsruhe Institute of Technology, 76021 Karlsruhe, Germany*
[5]*Department of Physics Engineering, Faculty of Engineering, Mie University, Tsu, Mie 514-8507, Japan*

Using time-resolved charge detection in a double quantum dot, we present an experimental test of the fluctuation theorem. The fluctuation theorem, a result from nonequilibrium statistical mechanics, quantifies the ratio of occurrence of fluctuations that drive a small system against the direction favored by the second law of thermodynamics. Here, these fluctuations take the form of single electrons flowing against the source–drain bias voltage across the double quantum dot. Our results, covering configurations close to as well as far from equilibrium, agree with the theoretical predictions, when the finite bandwidth of the charge detection is taken into account. In further measurements, we study a fluctuation relation that is a generalization of the Johnson–Nyquist formula and relates the second-order conductance to the voltage dependence of the noise. Current and noise can be determined with the time-resolved charge detection method. Our measurements confirm the fluctuation relation in the nonlinear transport regime of the double quantum dot. © *2013 American Institute of Physics.* [http://dx.doi.org/10.1063/1.4795540]

I. INTRODUCTION

The second law of thermodynamics states that the entropy of a macroscopic system out of equilibrium, when observed during a time τ, will exhibit a strictly positive change $\Delta S > 0$. This law is formulated in a framework of thermodynamic state variables which obey a deterministic evolution, and holds only in the limit of large systems and/or long times. The equivalently defined state variables of *small* systems on the other hand fluctuate in time and therefore do not fall within that framework. The charge flowing across a resistor, for example, is a stochastic quantity and is subject to the well-known Johnson–Nyquist fluctuations.[1,2] A great success in statistical mechanics has been the development of linear-response theory which allows to quantify such fluctuations for systems close to equilibrium. This theory originated in the discovery of general relations between the *equilibrium fluctuations* of a variable and its *linear response to a driving force*,[3–5] and was not least inspired by the findings of Johnson and Nyquist.

In the nonlinear regime far from equilibrium, these powerful tools cannot be applied. A remarkably simple extension of linear-response theory to the far-from-equilibrium regime has been found in the form of so-called fluctuation theorems (FTs) in the 1990s (Ref. 6) (although some results on nonlinear response date back earlier[7]).

We consider a situation as depicted in Fig. 1(a). We wish to describe the properties of a dissipative system X_{diss} coupled to a large bath X_{bath} at temperature T. The dissipative system is driven out of equilibrium by an external force. For clarity, we define a third system X_{drive} that plays this

role. In our example, X_{diss}, X_{drive}, and X_{bath} are a resistor, a battery, and their environment, respectively. We first consider the systems as macroscopic ones and assume X_{diss} to be in a steady state. During a sufficiently long time τ, the work δW performed on X_{diss} exactly balances with the heat δQ flowing out of it. The process is associated with a change $\Delta S = \delta Q/T$ of the entropy of $X_{drive} + X_{diss}$. Being in a steady state, the macrostate of X_{diss} is constant, and we can therefore attribute the entropy change ΔS entirely to X_{drive}. However, we can localize the *production* of entropy through dissipation inside X_{diss}.

In the next step, we allow for the system X_{diss} to be microscopic in the thermodynamic sense. The entropy production per time interval ΔS is then no longer unique, but fluctuates from one time interval to the next. These fluctuations are described with the help of a probability distribution function $P_\tau(\Delta S)$. In the most general wording, FTs state a relation of the form:

$$\frac{P_\tau(\Delta S)}{P_\tau(-\Delta S)} = e^{\Delta S/k_B}. \tag{1}$$

That is, the ratio of occurrences of system trajectories *producing* and *consuming* an entropy ΔS and $-\Delta S$, respectively, is given by a simple exponential factor.

A coarse classification of fluctuation theorems into transient and steady-state ones is possible based on the restrictions imposed upon the time τ.[8] Transient FT take into account changes of the state of X_{diss} and are valid for all $\tau > 0$. Steady-state FTs are valid only for $\tau \to \infty$. In this limit, the changes of the state of X_{diss} are negligible compared to the changes of the state of X_{drive}. An experimental test of a steady-state FT, as we present it here, needs to be

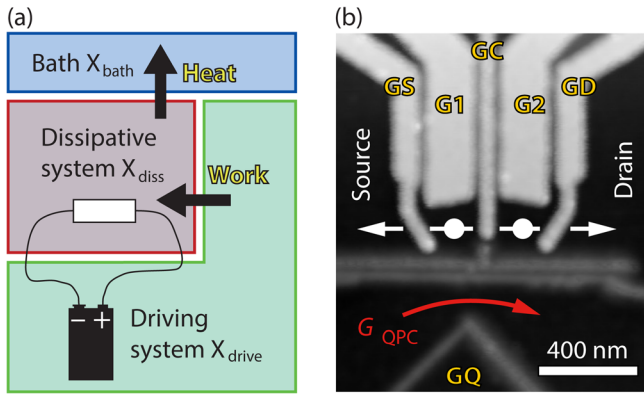a)Electronic address: kuengb@phys.ethz.ch

FIG. 1. (a) Configuration described by the FT. The essential part is a dissipative system (here, an electrical resistor) which is brought out of equilibrium by an external force (here a voltage) performing work. The dissipated heat flows into a thermal bath. (b) Atomic-force micrograph of the sample. Electrons can travel between the source and drain via the two quantum dots marked by disks. The conductance G_{QPC} of the quantum point contact serves to read out the charge state of the quantum dots. Fig. 1(b) reprinted with permission from Küng *et al.*, Phys. Rev. X **2**, 011001 (2012). Copyright (2012) by the American Physical Society.

carried out in a window in which τ is large enough to ensure the long-time limit, but short enough such that the accumulated entropy change ΔS is still comparable to k_B, and thus, the exponential in Eq. (1) remains measurable.

In the previous experimental work,[9–12] these conditions were realized in a number of classical systems operating at room temperature. Using single-electron transport devices at cryogenic temperatures opens, the possibility to enter a new regime in which the observed energy fluctuations are scaled down by more than three orders of magnitude. The measurements performed to date[13–15] have covered the classical regime, but pave the way for an experimental test of a quantum fluctuation theorem.[16–18]

In the experiment presented here,[14] we verify the fluctuation theorem for single-electron tunneling[19–21] by the technique of real-time charge detection[22,23] in a double quantum dot (DQD) coupled to source and drain electrodes in series. By monitoring the charge occupation of the DQD, we can determine the direction-resolved charge flow through this device.[24] The statistics of the charge flow corresponds to the statistics of ΔS in Eq. (1), and the electron counting method therefore allows for a test of the fluctuation theorem.

A recent experiment following this line[13] revealed the importance of back-action[25] of the charge sensing device, a quantum point contact[26] (QPC). Back-action due to nonequilibrium QPC noise destroys micro-reversibility in the DQD and leads to quantitative disagreement of the measurement and Eq. (1).[13,27,28] In order to avoid the spurious back-action, we employ an optimized sample design combining electron-beam and scanning-probe lithography[29] as shown in Fig. 1(b). It provides the high tunability and electronic stability required for the experiment while maintaining a good QPC–DQD coupling. We observe quantitative agreement between our data and theory in the near-equilibrium regime after including a small correction due to finite detector bandwidth,[30] which is a technical rather than physical complication and requires no fitting parameter. In the regime far from equilibrium, we

observe good agreement between experiment and theory in configurations where the DQD dynamics are those of a three-state Markovian system.

The single-electron counting technique gives us access to the DQD current and its noise.[31] This permits us to study a subject related to that of the FT, the subject of fluctuation relations between transport and noise coefficients. These relations are naturally derived from the FT as well as Onsager–Casimir and fluctuation–dissipation relations.[32,33] Here, we consider in particular fluctuation relations between second-order conductance (the second derivative of the current w.r.t. the source–drain voltage) and noise susceptibility (the first derivative of the zero-frequency noise spectral density w.r.t. the source–drain voltage). These were also the subject of a pioneering experimental work[34] performed by conventional noise measurements on an Aharonov–Bohm interferometer. It demonstrated a clear proportionality between second-order conductance and noise susceptibility, both in the even and odd parts in magnetic field as expected from theory.[32,33] Here, we pursue the investigation of this fluctuation relation in the regime of classical single-electron transport at zero magnetic field. By tuning our DQD to a regime with nonzero second-order conductance, we can test and quantitatively verify the theoretical predictions.

II. EXPERIMENTAL SETUP

Our measurements were performed in a ^{3}He/^{4}He dilution refrigerator on the sample shown in Fig. 1(b). The dark parts in the atomic-force micrograph correspond to the conductive (non-depleted) parts of a two-dimensional electron gas 34 nm below the surface of a GaAs/Al$_{0.3}$Ga$_{0.7}$As heterostructure (sheet density $n_S = 4.9 \times 10^{15}\,\text{m}^{-2}$, mobility $\mu = 33\,\text{m}^2/\text{Vs}$ as determined at $T = 4.2\,\text{K}$). Confinement is achieved in one part with Ti/Au gates (upper half of the image) biased with negative voltages. The thin vertical finger gates are only slightly biased in order to maintain a small tunneling coupling between the two QDs (white disks) and the source and drain leads. The horizontal lines are created by local anodic oxidation and electrically separate the DQD from the charge detector QPC in the lower half of the image. The detector's conductance G_{QPC} is sensitive to the charge on the DQD and abruptly decreases if an electron is loaded to either of the two QDs.

Tuning the voltages on gates G1 and G2, we reach a configuration with an estimated number of 80 electrons on each QD and close to the degeneracy of three DQD charge states with one excess electron on the left QD ("L"), or one on the right QD ("R"), or with no excess electron ("0"). By thermal excitation, the DQD rapidly jumps between these states, which we observe as a jumping of the charge detector signal G_{QPC} between three levels as shown in Fig. 2(a).

Each state change corresponds to an electron passing one of the barriers underneath the gates near source (GS), near drain (GD), or at the center of the structure (GC) as indicated in the diagram in Fig. 2(b). (Anti)clockwise transitions in this diagram correspond to electron transfer towards the drain (source). To measure the net number n of electrons having transferred one barrier, we keep track of the number
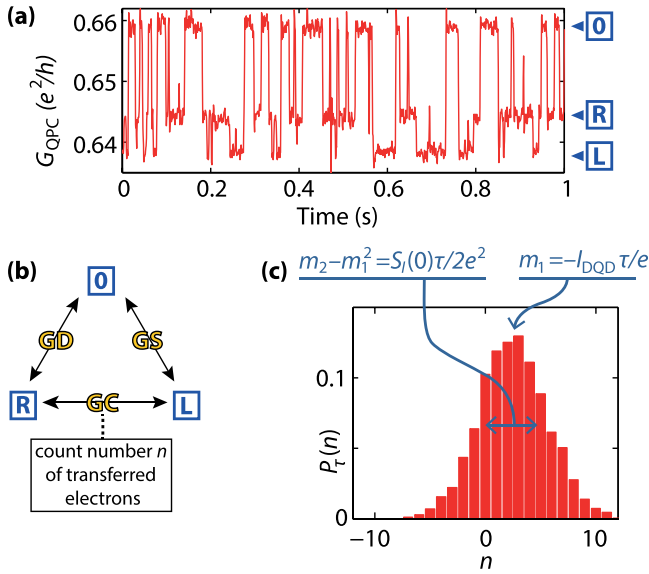
FIG. 2. (a) G_{QPC} time trace recorded at a positive DQD source–drain voltage. The three discrete levels are assigned to the DQD charge states L, R, and 0. (b) Diagram of the DQD states and transitions. To count the number n of electrons that pass the center DQD barrier, we count the number of transitions L $\rightarrow$ R minus R $\rightarrow$ L. (c) Histogram of the electron number n obtained from the analysis of 3000 time segments of length $\tau = 2$ s. The histogram was measured at finite DQD source–drain voltage $V_{DQD} = 20\,\mu$V and has a nonzero mean value $\langle n \rangle$ which converts into a nonzero DQD current I_{DQD}. The variance of the histogram, $m_2 - m_1^2$, determines the zero-frequency current noise spectral density S_I of the DQD. Fig. 2(a) reprinted with permission from Küng *et al.*, Phys. Rev. X **2**, 011001 (2012). Copyright (2012) by the American Physical Society.

of corresponding level transitions in the detector signal during a time τ. In our case, we choose the barrier GC and count the number of transitions L $\rightarrow$ R minus the number of transitions R $\rightarrow$ L. If τ is large compared to the typical dwell time of an electron inside the DQD, the electron passing the center barrier will typically reach one of the leads where it equilibrates with the thermal bath at temperature T. Then each n categorizes a set of system trajectories with equal energy dissipation neV_{DQD} which can be positive or negative depending on the direction of the charge flow with respect to the direction of the source–drain voltage V_{DQD}. Correspondingly, the entropy production is given by $\Delta S = neV_{DQD}/T$ and the FT for our system[18,21,33] reads

$$\frac{P_\tau(n)}{P_\tau(-n)} = e^{neV_{DQD}/k_BT}. \qquad (2)$$

III. TEMPERATURE DEPENDENCE

In Fig. 2(c), we show an experimentally determined histogram $P_\tau(n)$ as it is appearing in Eq. (2). The histogram is based on the counting analysis of 3000 G_{QPC} time segments each with length $\tau = 2$ s and was measured at an electronic temperature of $T = 330$ mK. The choice of τ is such to minimize the combined error originating from the imperfect long-time limit[13,18,21,33] (favoring large τ) and from statistics (favoring small τ). The histogram was obtained at a source–drain bias of $V_{DQD} = 20\,\mu$V and features a nonzero mean value $\langle n \rangle \equiv m_1$ corresponding to a nonzero average DQD current $I_{DQD} = em_1/\tau$. Here, we have introduced the notion

m_k for the k-th moment of $P_\tau(n)$. The variance $m_2 - m_1^2$ of the histogram is proportional to the noise in I_{DQD}—we will come back to this point in the discussion of the fluctuation relations. Despite the positive average m_1, for some of the time segments, charge flow is against the applied bias ($n < 0$), which results in a temporary *decrease* of the system entropy.

Measurements like the one in Fig. 2(c) were carried out at temperatures 500 mK and 700 mK to test the temperature dependence of Eq. (2). In addition to these measurements at $V_{DQD} = 20\,\mu$V, measurements at $V_{DQD} = 0\,\mu$V served to check the behavior of the system in equilibrium. This set of data is shown in Figs. 3(a)–3(c), where the data points are the natural logarithm of the left-hand side of Eq. (2) measured at $V_{DQD} = 0\,\mu$V and $V_{DQD} = 20\,\mu$V, respectively. The expression $\ln[P_\tau(n)/P_\tau(-n)]$ follows the expected linear behavior close to the theoretical curve neV_{DQD}/k_BT (solid lines).

IV. FINITE-BANDWIDTH CORRECTION

In the non-zero bias case, there is a systematic deviation of 20%–30% in the slope. This can be understood by taking into account the limited bandwidth of the charge detection. A charge switching event in the DQD is detected in the QPC only after a reaction time of $1/\Gamma_{det}$, which in our case is determined both by the bandwidth of the measurement electronics and by the details of the analysis algorithm. If the charge state switches back too fast, the event is missed. Following ideas of Ref. 35, Utsumi *et al.*[30] calculated the
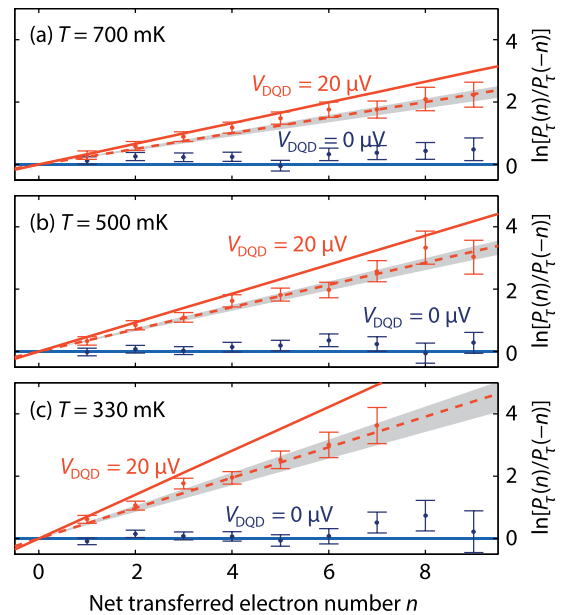

FIG. 3. (a)–(c) Comparison of experimental data with theory for three different bath temperatures. The data points correspond to the left-hand side of Eq. (2) and describe the probability ratio of forward (+n, entropy-producing) and backward (−n, entropy-consuming) processes for a given n. The solid lines mark the expected exponential behavior $\exp(neV_{DQD}/k_BT)$ for the two source–drain voltages 0 μV (dark blue) and 20 μV (red). If the finite bandwidth of the detector is taken into account[30,35] (dashed lines), experiment and theory agree within the statistical uncertainty of the data (error bars: estimated standard deviation). Reprinted with permission from Küng *et al.*, Phys. Rev. X **2**, 011001 (2012). Copyright (2012) by the American Physical Society.

effect of the finite bandwidth and found that to leading order it can be incorporated in a correction factor $\alpha_{BW} < 1$ to the term eV_{DQD}/k_BT, just like observed in our experiment. The factor $\alpha_{BW} = k_BT\ln w^*/eV_{DQD}$ is expressed in terms of the six transition rates Γ_{ij} between the states $i, j = L, R, 0$

$$w^* \approx w + \frac{1-w}{\Gamma_{det}}\left(\frac{\Gamma_{L0}\Gamma_{0R}}{\Gamma_{LR}} + \frac{\Gamma_{RL}\Gamma_{L0}}{\Gamma_{R0}} + \frac{\Gamma_{0R}\Gamma_{RL}}{\Gamma_{0L}}\right), \quad (3)$$

where $w = \exp(eV_{DQD}/k_BT)$. Qualitatively, the effect can be understood as follows. At a nonzero bias, transitions directed towards drain occur with faster rates ($\Gamma_{L0}, \Gamma_{RL}, \Gamma_{0R}$) than those directed towards source ($\Gamma_{0L}, \Gamma_{LR}, \Gamma_{R0}$). It is therefore more likely that the detector misses a charge flowing towards drain than towards source, i.e., the ratio $P_\tau(n)/P_\tau(-n)$ decreases for $n > 0$.

The detection rate $\Gamma_{det} = (0.59\pm0.12)$ kHz is given by the inverse of the shortest lifetime of a charge state that can be detected by our setup. The rates Γ_{ij} appearing in Eq. (3) were determined directly from the charge detection signal as described in Ref. 24. The dashed lines in Figs. 3(a)–3(c) show the theoretical expectation calculated with these parameters, indeed agreeing much better with the experiment. The gray shaded areas indicate the uncertainty in the slope which mainly reflects the uncertainty in Γ_{det}. We emphasize that this analysis does not involve any free parameters.

The QPC back-action and the finite bandwidth affect the measured *data* in a similar way. However, the implications for the measured *system* are very different. QPC back-action implies an influence of the measurement device on the measured system, whereas for the finite detection bandwidth there is no such influence. In our case, the absence of QPC back-action is most strongly supported by the data obtained at zero $V_{DQD} = 0\,\mu$V in Fig. 3. Independently of the predictions of the FT, we expect a distribution $P_\tau(n)$ that is symmetric about $n = 0$ (i.e., $\ln[P_\tau(n)/P_\tau(-n)] = 0$) at $V_{DQD} = 0\,\mu$V. Back-action effects are expected to break this symmetry because of rectification, which is a generic consequence of the left–right asymmetry of the sample.[36,37] A further independent test is the dependence of the measured distributions on the QPC source–drain voltage (not shown). The dependencies expected in the presence of QPC back-action, namely, a shift of the mean m_1 (due to rectification) and an increase of the variance $m_2 - m_1^2$ (due to excess noise) were absent for QPC source–drain voltages below $600\,\mu$V.

V. HIGH-BIAS REGIME

The DQD voltage of $20\,\mu$V used in the temperature-dependence measurements is comparable with the thermal voltage $k_BT/e = 28$–$58\,\mu$V, so the system is not too far from thermal equilibrium. The FT however also applies far away from equilibrium. To test its predictions in this regime, we performed bias-dependence measurements with V_{DQD} up to $120\,\mu$V, i.e., about $4.3 \times k_BT/e$ at $T = 330$ mK. The data are shown in Fig. 4 and is based on the analysis of 2000 G_{QPC} time segments of length $\tau = 2$ s for each DQD voltage. For clarity and to reduce the statistical error for large voltages, we plot an integrated version of Eq. (2) relating the
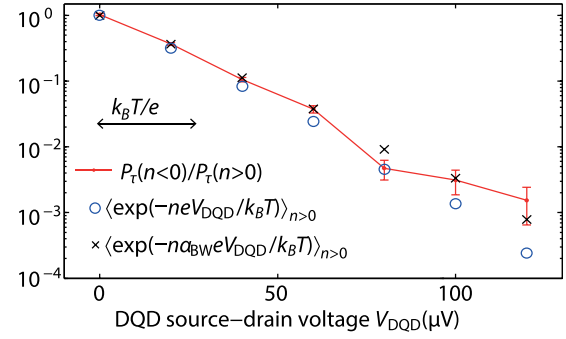

FIG. 4. The red data points show the V_{DQD}-depencence of the left-hand side of Eq. (4), the ratio of entropy-consuming vs. entropy-producing cycles, with error bars indicating its estimated standard deviation. The blue circles show the right-hand side, the average of the Boltzmann factor among the entropy-consuming cycles. The FT (4) is satisfied if the finite detector bandwidth is taken into account in the form of a correction factor α_{BW} to the exponent in Eq. (4) (crosses). The uncertainty in the finite-bandwidth correction is comparable with the error on $P_\tau(n < 0)/P_\tau(n > 0)$ for all bias voltages. Reprinted with permission from Küng *et al.*, Phys. Rev. X **2**, 011001 (2012). Copyright (2012) by the American Physical Society.

total fractions of entropy-producing and entropy-consuming cycles

$$\frac{\sum_{n<0}P_\tau(n)}{\sum_{n>0}P_\tau(n)} = \frac{\sum_{n>0}P_\tau(n)e^{-neV_{DQD}/k_BT}}{\sum_{n>0}P_\tau(n)}. \quad (4)$$

The red data points in Fig. 4(a) are the left-hand side of Eq. (4). It rapidly decreases with DQD voltage, as charge transfer against the bias occurs less and less frequently. The blue circles are the right-hand side, calculated without finite-bandwidth correction. Similar to the low-bias case, there is a systematic deviation between the two which can be fully ascribed to the finite bandwidth of the detection. Namely, the data shown as black crosses correspond to a bandwidth-corrected version of the right-hand side of Eq. (4) for which the exponent $-neV_{DQD}/k_BT$ was replaced by $-\alpha_{BW}neV_{DQD}/k_BT$.

Measurements at even higher DQD voltages are eventually limited by the necessary, exponentially increasing measurement time. The duration of measurement series as the one shown in Fig. 4 was in our case limited by the occurrence, roughly once per day, of small charge rearrangements in the vicinity of the DQD. These rearrangements would alter the potential landscape of the DQD by values of order $10\,\mu$V. They could be detected in the form of discontinuities in the measured data, and of gate voltage shifts of the DQD stability diagram before and after the measurement. Higher measurement precision can be achieved equivalently by increasing the measurement time (i.e., improving sample stability) and by increasing the measurement speed (i.e., improving the bandwidth of the charge detection).

VI. FLUCTUATION RELATIONS

We now turn to the fluctuation relations discussed shortly in the Introduction. Generally, we are speaking about relations among Taylor coefficients (with respect to source–drain voltage) of the moments

$$m_k = \sum_n n^k P_\tau(n) \qquad (5)$$

of the distribution $P_\tau(n)$. Here, we study the two lowest-order fluctuation relations at zero magnetic field. These involve the moments m_1 and m_2 and their derivatives. The moments have direct relations with the electrical current through the DQD, $I_{DQD} = -em_1/\tau$, and with the zero-frequency noise spectral density, $S_I = 2e^2(m_2 - m_1^2)/\tau$. In contrast to conventional noise measurements,[34] measuring the noise and current by electron counting requires no calibration of the signal amplification and no subtraction of an offset, and therefore, is particularly well suited for a quantitative experiment.

The fluctuation relations of interest read

$$S_I = 4k_B T \left.\frac{dI(V_{DQD})}{dV_{DQD}}\right|_{V_{DQD}=0}, \qquad (6)$$

$$\left.\frac{dS_I(V_{DQD})}{dV_{DQD}}\right|_{V_{DQD}=0} = 2k_B T \left.\frac{d^2 I(V_{DQD})}{dV_{DQD}^2}\right|_{V_{DQD}=0}. \qquad (7)$$

The first relation, Eq. (6), is the well-known Johnson–Nyquist formula for the equilibrium noise. The second relation, Eq. (7), goes beyond the equilibrium properties of the conductor and relates the nonequilibrium noise to the nonlinearity of the I/V characteristic.

In contrast to the measurements shown in Secs. V and III which were individually completed at fixed configurations of gate and source–drain voltages, measuring the coefficients appearing in Eqs. (6) and (7) requires us to record the source–drain voltage dependence of the distribution $P_\tau(n)$. In order to measure a nontrivial fluctuation relation (7), an I/V characteristic with a sufficiently strong nonlinearity is needed. The measurements presented in Secs. III and V were performed in configurations close to the charge degeneracy point where the I/V characteristic is rather linear. In moving away from the degeneracy point, the nonlinearity is increased due to the rectifying effect of the DQD. On the other hand, by that we tune the DQD further into Coulomb blockade and reduce its overall conductance. Because this means that fewer charging events per second are counted, moving away from the degeneracy point conflicts with the requirement to acquire large statistical samples.

Considering the results of Sec. III, we must expect that the measurements of the source–drain voltage dependence of m_1 and m_2 are influenced by the finite detector bandwidth. We carried out a numerical evaluation of the model of Ref. 30 to determine the corrections Δm_k to be subtracted from the measured moments m_k^*. (For details of this calculation, see Ref. 38.)

In Fig. 5, we show the quantitative comparison between experiment and theory. In the upper plot, we show the bandwidth-corrected $I_{DQD} = e(m_1^* - \Delta m_1)/\tau$ along with a fit to a second-order polynomial in V_{DQD} from which we determined the first- and second-order conductance. Fitting to a polynomial of third, fourth, and fifth degree did not yield significantly different coefficients. First- and second-order conductance were inserted into the fluctuation relations (6) and (7) to determine the expected linear dependence of S_I on
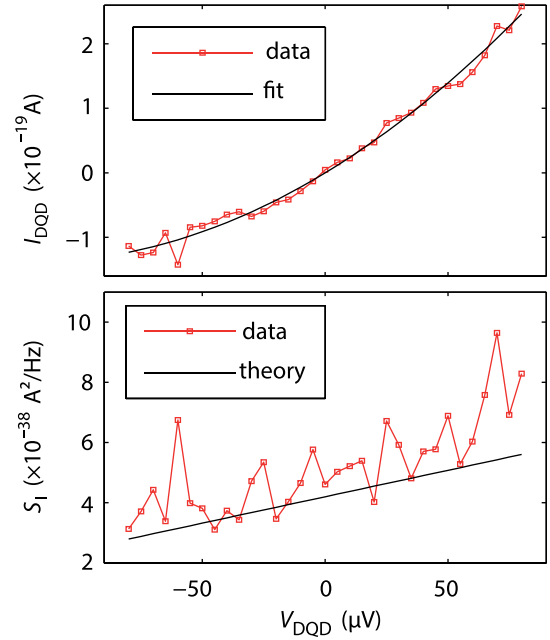

FIG. 5. Measurement of fluctuation relation between DQD current and noise. The upper plot shows the bandwidth-corrected DQD current ($\tau = 10$ s, 260 time bins per point) along with a fit to a second-order polynomial in V_{DQD}. Using the linear and quadratic coefficients of the fit, the fluctuation relations (6) and (7) are used to calculate the expected (linear) dependence of S_I on V_{DQD}. This is plotted as a black line along with the data in the lower plot.

V_{DQD}. Only the measured temperature $T = 330$ mK enters as an additional parameter. The calculation is plotted in the lower graph along with the bandwidth-corrected data for the noise, $S_I = 2e^2[(m_2^* - \Delta m_2) - (m_1^* - \Delta m_1)^2]$. Comparison between the two demonstrates that the fluctuation relations quantitatively explain the dependence of the noise on bias based on the properties of the I/V characteristic. In particular, the special property of the noise to drop below the thermal equilibrium noise at negative V_{DQD} originates in a nonzero second-order conductance.[34]

VII. CONCLUSION

In conclusion, we presented an experimental test of the fluctuation theorem and fluctuation relations for single-electron transport through a DQD. Our data on the fluctuation theorem cover different temperatures and a large range of source–drain voltages and are in good agreement with theory. Our data on fluctuation relations consist of a measurement of the bias dependence of the current and current noise of the DQD by means of single-electron counting. The data permit to test and verify a generalization of the Johnson–Nyquist formula, an exact relation between second-order conductance and voltage-linear part of the noise. Combining a sensitivity to individual thermal fluctuations with sub-Kelvin temperatures, our results demonstrate the good control over thermal (non)equilibrium required for future tests of the fluctuation theorem in quantum transport.

[1]J. B. Johnson, Phys. Rev. **32**, 97 (1928).
[2]H. Nyquist, Phys. Rev. **32**, 110 (1928).
[3]H. B. Callen and T. A. Welton, Phys. Rev. **83**, 34 (1951).
[4]M. S. Green, J. Chem. Phys. **20**, 1281 (1952).
[5]R. Kubo, J. Phys. Soc. Jpn. **12**, 570 (1957).
[6]D. J. Evans, E. G. D. Cohen, and G. P. Morriss, Phys. Rev. Lett. **71**, 2401 (1993).
[7]G. Bochkov and Y. E. Kuzolev, Zh. Eksp. Teor. Fiz. **72**, 238 (1977).
[8]D. J. Evans and D. J. Searles, Adv. Phys. **51**, 1529 (2002).
[9]G. M. Wang, E. M. Sevick, E. Mittag, D. J. Searles, and D. J. Evans, Phys. Rev. Lett. **89**, 050601 (2002).
[10]N. Garnier and S. Ciliberto, Phys. Rev. E **71**, 060101 (2005).
[11]D. Collin, F. Ritort, C. Jarzynski, S. B. Smith, I. Tinoco, Jr., and C. Bustamante, Nature (London) **437**, 231 (2005).
[12]S. Schuler, T. Speck, C. Tietz, J. Wrachtrup, and U. Seifert, Phys. Rev. Lett. **94**, 180602 (2005).
[13]Y. Utsumi, D. S. Golubev, M. Marthaler, K. Saito, T. Fujisawa, and G. Schön, Phys. Rev. B **81**, 125331 (2010).
[14]B. Küng, C. Rössler, M. Beck, M. Marthaler, D. S. Golubev, Y. Utsumi, T. Ihn, and K. Ensslin, Phys. Rev. X **2**, 011001 (2012).
[15]O.-P. Saira, Y. Yoon, T. Tanttu, M. Mttnen, D. Averin, and J. P. Pekola, Phys. Rev. Lett. **109**, 180601 (2012).
[16]J. Kurchan, e-print: arXiv:cond-mat/0007360v2.
[17]H. Tasaki, e-print: arXiv:cond-mat/0009244v2.
[18]M. Esposito, U. Harbola, and S. Mukamel, Rev. Mod. Phys. **81**, 1665 (2009).
[19]J. Tobiska and Y. V. Nazarov, Phys. Rev. B **72**, 235328 (2005).
[20]D. Andrieux and P. Gaspard, J. Stat. Mech.: Theory Exp. **2006**, P01011.
[21]M. Esposito, U. Harbola, and S. Mukamel, Phys. Rev. B **75**, 155316 (2007).
[22]L. M. K. Vandersypen, J. M. Elzerman, R. N. Schouten, L. H. Willems van Beveren, R. Hanson, and L. P. Kouwenhoven, Appl. Phys. Lett. **85**, 4394 (2004).
[23]R. Schleser, E. Ruh, T. Ihn, K. Ensslin, D. C. Driscoll, and A. C. Gossard, Appl. Phys. Lett. **85**, 2005 (2004).
[24]T. Fujisawa, T. Hayashi, R. Tomita, and Y. Hirayama, Science **312**, 1634 (2006).
[25]S. Gustavsson, M. Studer, R. Leturcq, T. Ihn, K. Ensslin, D. C. Driscoll, and A. C. Gossard, Phys. Rev. Lett. **99**, 206804 (2007).
[26]M. Field, C. G. Smith, M. Pepper, D. A. Ritchie, J. E. F. Frost, G. A. C. Jones, and D. G. Hasko, Phys. Rev. Lett. **70**, 1311 (1993).
[27]G. Bulnes Cuetara, M. Esposito, and P. Gaspard, Phys. Rev. B **84**, 165114 (2011).
[28]D. S. Golubev, Y. Utsumi, M. Marthaler, and G. Schön, Phys. Rev. B **84**, 075323 (2011).
[29]C. Rössler, B. Küng, S. Dröscher, T. Choi, T. Ihn, K. Ensslin, and M. Beck, Appl. Phys. Lett. **97**, 152109 (2010).
[30]Y. Utsumi, D. S. Golubev, M. Marthaler, T. Fujisawa, and G. Schön, in *Perspectives of Mesoscopic Physics-dedicated to Joseph Imry's 70th Birthday*, edited by A. Aharoni and O. Entin-Wohlman (World Scientific, 2010), pp. 397–414.
[31]S. Gustavsson, R. Leturcq, B. Simovic, R. Schleser, T. Ihn, P. Studerus, K. Ensslin, D. C. Driscoll, and A. C. Gossard, Phys. Rev. Lett. **96**, 076605 (2006).
[32]H. Förster and M. Büttiker, Phys. Rev. Lett. **101**, 136805 (2008).
[33]K. Saito and Y. Utsumi, Phys. Rev. B **78**, 115429 (2008).
[34]S. Nakamura, Y. Yamauchi, M. Hashisaka, K. Chida, K. Kobayashi, T. Ono, R. Leturcq, K. Ensslin, K. Saito, Y. Utsumi *et al.*, Phys. Rev. Lett. **104**, 080602 (2010).
[35]O. Naaman and J. Aumentado, Phys. Rev. Lett. **96**, 100201 (2006).
[36]V. S. Khrapai, S. Ludwig, J. P. Kotthaus, H. P. Tranitz, and W. Wegscheider, Phys. Rev. Lett. **97**, 176803 (2006).
[37]U. Gasser, S. Gustavsson, B. Küng, K. Ensslin, T. Ihn, D. C. Driscoll, and A. C. Gossard, Phys. Rev. B **79**, 035303 (2009).
[38]B. Küng, Ph.D. dissertation, ETH Zurich, 2012.